Available online at www.sciencedirect.com
SCIENCE DIRECT®
Journal of Hydrology 276 (2003) 89–111
Journal of Hydrology
www.elsevier.com/locate/jhydrol

Effect of geomorphologic resolution on modeling of runoff hydrograph and sedimentograph over small watersheds

Latif Kalin[a,b], Rao S. Govindaraju[a,*], Mohamed M. Hantush[b]

[a]US EPA, National Risk Management Research Laboratory, Cincinnati, OH 45268, USA
[b]Purdue University, Department of Civil Engineering, School of Civil Engineering, 1284 Civil Engineering Bldg, West Lafayette, IN 47907, USA

Received 7 January 2002; accepted 21 January 2003

Abstract

In hydrologic models, Geographic Information Systems (GIS) interfaces are commonly used for extracting the channel network, and delineating the watershed. By overlaying soil and land use maps onto the extracted channel network, input files required by the model are prepared. However, the nature of the extracted channel network strongly depends on some pre-selected threshold values within the GIS framework, which in turn, determine the geomorphologic resolution. There are no accepted guidelines for selecting these threshold parameters making the extraction of channel networks a subjective process. In this study, we investigate the effect of geomorphologic resolution on runoff hydrographs and sedimentographs over two small USDA experimental watersheds. The KINEROS model with ArcView interface has been used for this purpose. An empirical relationship between optimal resolution, watershed characteristics and nature of the storm has been developed. Results reveal that geometric simplification of the watershed for rainfall-runoff-erosion studies may be acceptable under right combinations of rainfall events and watershed properties. Our results also indicate that the optimal geomorphologic resolution may not be the same for hydrographs and sedimentographs.

Keywords: Geographic information systems; Models; Surface water; Soil erosion

1. Introduction

Estimating direct runoff and sediment yield from a watershed is important both from water quantity and quality standpoints. In this regard, the use of distributed hydrologic models has gained wider acceptance over lumped models because of their ability to handle spatial variability of both climatic and topographic parameters. However, distributed models tend to be more complex and typically need a large number of parameters that need to be estimated or measured. As the spatial scale of the catchment increases, modeling hydrologic processes of rainfall-runoff and surface erosion become more complex. A greater number of sub-watersheds, while improving accuracy, increases the input data preparation effort and the subsequent computational effort.

* Corresponding author. Address: Purdue University, Department of Civil Engineering, School of Civil Engineering, 1284 Civil Engineering Bldg, West Lafayette, IN 47907, USA. Fax: +1-765-496-1988.
E-mail addresses: govind@ecn.purdue.edu (R.S. Govindaraju), kalin.latif@epamail.epa.gov (L. Kalin), hantush.mohamed@epamail.epa.gov (M.M. Hantush).

0022-1694/03/$ - see front matter © 2003 Elsevier Science B.V. All rights reserved.
doi:10.1016/S0022-1694(03)00072-6

Studies on the influence of catchment scale on hydrologic response can be traced back to the early 1960's (Minshall, 1960; Amorocho, 1961) and, since then, many methods and models have been investigated to reduce the complexity that arises from distributed modeling of watersheds (Kirkby, 1988; Moore et al., 1988). Several studies (Norris, 1992; Norris and Haan, 1993; Goodrich et al., 1988) concluded that for a given rainfall event, increasing the number of subwatersheds beyond a certain point did little to improve model results. Similar conclusions were reached by Corradini et al. (1986) when using basin order to quantify spatial scale. Using the concept of equilibrium storage, Goodrich (1992) found that an average first order channel support area of approximately 14% of total basin area provides a discretization level for adequate model performance for most applications.

Currently, watershed delineation and stream network extraction are accomplished by utilizing Geographic Information Systems (GIS) and Digital Elevation Models (DEMs). The most common method of extracting channel networks is by specifying a critical source area (CSA) required for initiating a channel. However, the results after extraction are very sensitive to this threshold value (Morris and Heerdegen, 1988; Helmlinger et al., 1993; Montgomery and Foufoula-Georgiou, 1993). The specification of the CSA has been based on geomorphologic laws (Tarboton et al., 1991), scaling invariance of probability distributions of channel network attributes (Tarboton et al., 1988; Rodriguez-Iturbe et al., 1992; Rinaldo et al., 1992; Rigon et al., 1993), local slope (Montgomery and Dietrich, 1988), critical shear stress (Rinaldo et al., 1995) and terrain curvature (Tarboton and Ames, 2001).

Some studies have used both geomorphologic properties and hydrologic responses for determining CSAs (Helmlinger et al., 1993; Gandolphi and Bischetti, 1997). However, the assumptions of constant threshold areas and how they are influenced by morphometric and scaling properties are often not met in natural watersheds (Snell and Sivapalan, 1994; Da Ros and Borga, 1997).

Another approach to identify the appropriate CSA for channel extraction is based on the use of hydrologic models. For instance, Thieken et al. (1999) utilized the KINEROS model (Woolhiser et al., 1990) to evaluate data aggregation on watershed response from synthetic rainfall events. Zhang and Montgomery (1994) suggested a spatial resolution of 10 m to represent hydrologic processes based on simulations with TOPMODEL (Beven and Kirkby, 1979). Somewhat varying results were reported by Garbrecht and Martz (1996) and Bruneau et al. (1995). Bloschl and Sivapalan (1995) stated that high resolution DEMs are required when small-scale processes are dominant. Miller et al. (1999) showed that smaller watersheds are more sensitive to DEM resolution.

All of the above studies analyzed the impact of watershed subdivision or the selection of the threshold area on runoff hydrograph alone, and did not consider sediment yield. Goodrcih et al. (1988) claimed that geometric simplifications are unlikely when modeling sediment or chemical transport. Bingner et al. (1997) evaluated the effect of various levels of watershed subdivision and sub-watershed size on simulated annual sediment yield of fine material based on simulations with the SWAT model. They reported a minimal improvement in prediction of annual sediment yield beyond a certain number subwatersheds. Vieux and Needham (1993) investigated the sensitivity of a nonpoint-pollution model (AGNPS) to grid cell size. They found that grid cell size is the most important factor affecting sediment yield. As the cell size increases, channel stream meanders are short-circuited and sediment yield increases as a result. Previous studies with hydrologic models did not propose a quantifiable methodology to simplify the basin geometry, nor did they investigate this aspect when sediment transport was involved. In this regard, the main goals of this study are

- to develop a quantitative relationship between peak runoff, basin characteristics, and nature of the storm for single events.
- to analyze the effect of geometric simplification of the watershed on the peak sediment discharge and total sediment load measured at the outlet of the catchment.

The focus of this study is on large storms where we assume that most of the eroded sediment reaches the watershed outlet. It is hypothesized that there exists an optimal threshold of geomorphologic resolution,

beyond which subdividing the watershed further does not improve model performance significantly. Specifically, the role of geomorphologic resolution on runoff hydrograph, sedimentograph (sediment discharge vs time) and total sediment load is examined. Two experimental watersheds are utilized to validate this hypothesis. Runoff hydrographs and sedimentographs are generated using the KINEROS model (Woolhiser et al., 1990) with different resolutions to replicate observations over several storms on the watersheds. Based on results from several simulations, expressions for geomorphologic resolution are developed. Criteria for selecting the appropriate level of geomorphologic detail required for modeling surface water and sediment movement over watersheds is presented.

2. Study watersheds and data sources

Two experimental, field scale watersheds (namely W-2 and W-3) located near Treynor, IA with areas of approximately 83 and 107 acres (33 and 42 ha), respectively (Fig. 1), were utilized for this study. These watersheds are part of four experimental watersheds (W-1, W-2, W-3 and W-4) established by the US Department of Agricultural Research Service (USDA-ARS) in 1964 to determine the affect of various soil conservation practices on runoff and water-induced erosion (Figs. 2 and 3). This goal was accomplished by measuring runoff, baseflow, and sediment load using weirs located at the base of each of these watersheds.

Watersheds W-2 and W-3 are similar in characteristics with a rolling topography defined by gently sloping ridges, steep side slopes, and alluvial valleys with incised channels that normally end at an active gully head, typical of the deep loess soil in MLRA 107 (Kramer et al., 1990). Slopes usually change from 2 to 4 percent on the ridges and valleys and 12 to 16 percent on the side slopes. An average slope of about 8.4 percent is estimated for both watersheds, using first-order soil survey maps. The major soil types are well drained Typic Hapludolls, Typic Udorthents, and Cumulic Hapludolls (Marshall-Monona-Ida and Napier series), classified as fine-silty, mixed, mesics. The surface soils consist of silt loam and silty loam textures that are very prone to erosion, requiring suitable conservation practices to prevent serious erosion (Chung et al., 1999).

The cropped portions of the watersheds cover the ridges, side-slopes and toe-slopes. Bromegrass was maintained on the major drainage ways of the alluvial valleys. Corn has been grown continuously on W-2 since 1964, and on W-3 since 1972. The W-3 watershed was predominantly bromegrass with small amounts of orchardgrass and alfalfa from 1964 to 1971. These watersheds have been the subject of watershed-studies by many researchers for almost 30 years and numerous papers have been published regarding these watersheds (for, e.g. Karlen and Kramer, 1991; Karlen et al., 1998; Steinheimer et al., 1998a,b).

Larry Kramer (personal communication) at USDA-ARS National Tilt Laboratory, Iowa, provided runoff and sediment data which covers a 30 year time span from 1964 to 1993 with more than 500 rainfall events. Depending on the intensity and duration of the rainfall events, most of the data has been recorded at 1 min intervals. Such a fine temporal resolution is

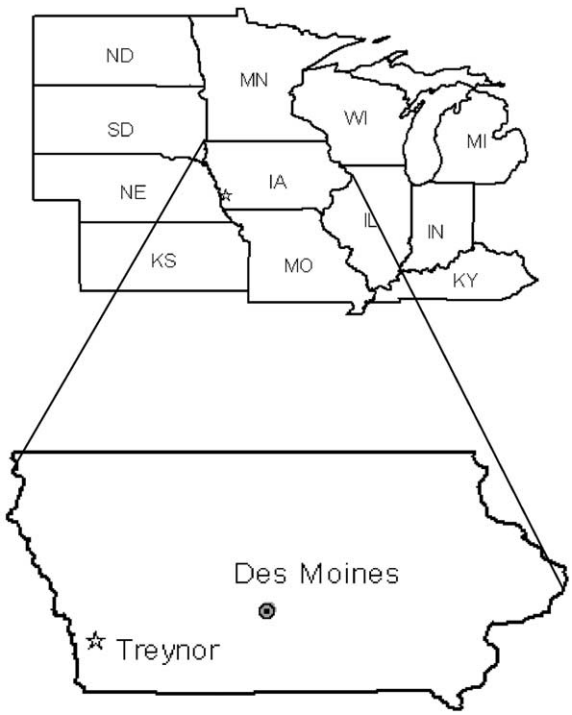

Fig. 1. Location of watersheds W-2 and W-3 near Treynor, IA.

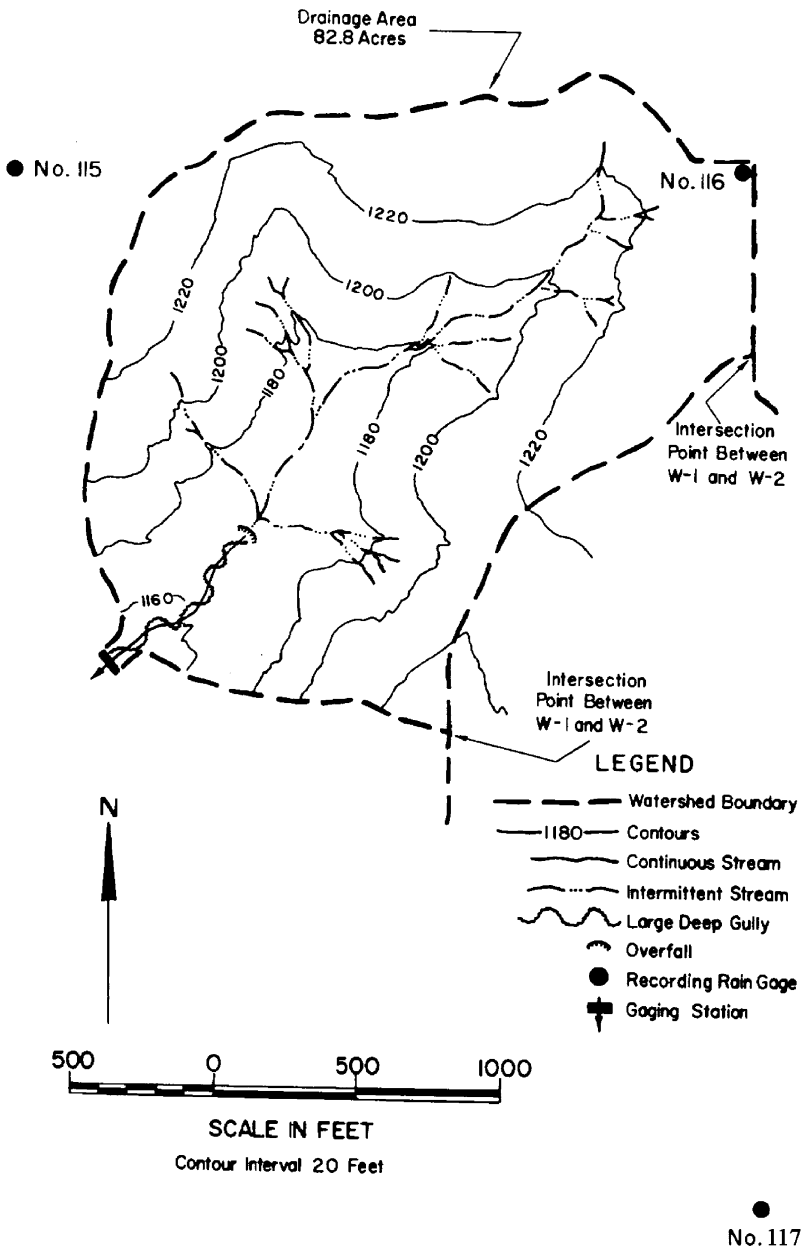

Fig. 2. Topography of watershed W-2 (adapted from ARS-USDA, http://hydrolab.arsusda.gov/wdc/ia.htm).

very useful for the purposes of this study and is not usually available. There are three rain gauges located around each watershed, rain gauges 112, 113 and 114 around W-3 and 115, 116 and 117 around W-2, as shown in Figs. 2 and 3. However, data for rain gauge 114 was not available. There are differences in measured precipitation between rain gauges during some events due to spatial and temporal variations even at such small scales. DEM data with 5 m horizontal and 10 cm vertical resolutions (1 m vertical

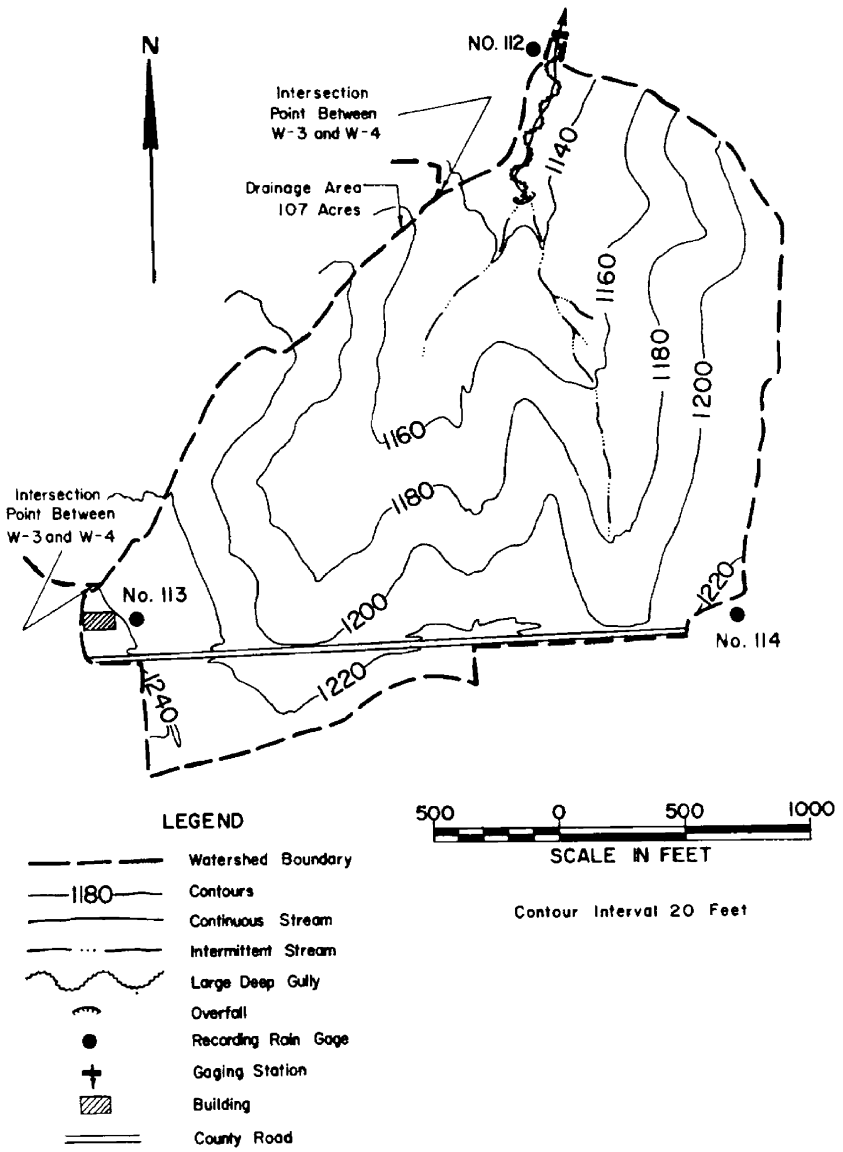

Fig. 3. Topography of watershed W-3 (adapted from ARS-USDA, http://hydrolab.arsusda.gov/wdc/ia.htm).

accuracy) was available which was generated from high resolution GPS data by USDA-ARS National Tilt Laboratory personnel.

3. Model description

The model KINEROS, developed by Woolhiser et al. (1990), was selected as the watershed model to be used during this study. It is a distributed, event based, deterministic and physically based model. This model is primarily useful for predicting surface runoff and erosion over small agricultural and urban watersheds. Runoff is calculated based on the Hortonian approach and infiltration is calculated by Smith and Parlange (1978) infiltration model. KINEROS requires the watershed to be divided into homogeneous overland flow planes and channel

segments, and models water movement over these elements in a cascading fashion. One-dimensional flow discharge per unit width, Q, is expressed in terms of the storage of water per unit area, h (= depth for a plane surface), through the kinematic approximation

$$Q = \alpha h^m \tag{1}$$

where α and m are parameters related to the slope s, roughness, and nature of flow. The continuity equation for upland areas is

$$\frac{\partial h}{\partial t} + \frac{\partial Q}{\partial x} = q(x,t) \tag{2}$$

where t is time, x is the spatial coordinate, and q is the net lateral inflow rate. The upstream condition is determined by the flow entering at the upstream end. The continuity equation for one-dimensional flow in channels is

$$\frac{\partial A}{\partial t} + \frac{\mathrm{d}Q}{\mathrm{d}A}\frac{\partial A}{\partial x} = q_c(x,t) \tag{3}$$

where A is flow cross-sectional area, Q is now channel discharge, and q_c is the net lateral inflow per unit length of channel. Under the kinematic wave approximation, Q in Eq. (3) is

$$Q = \alpha R^{m-1} A \tag{4}$$

where R is hydraulic radius. In Eqs. (1) and (4) $\alpha = \sqrt{s}/n$, $m = 5/3$ under Manning's equation, n is Manning's roughness coefficient, and s is slope. Channel sections may be approximated as being trapezoidal or circular. The upstream boundary is dictated by the amount of flow entering the channel. A four-point difference scheme is used for numerical discretization, and the resulting non-linear equations are solved using the Newton–Raphson method.

KINEROS accounts for erosion resulting from raindrop energy and by flowing water separately. A mass balance equation is solved to describe sediment dynamics at any point along a surface flow path

$$\frac{\partial}{\partial t}(AC_s) + \frac{\partial}{\partial x}(QC_s) - e(x,t) = q_s(x,t) \tag{5}$$

where C_s is volumetric sediment concentration, e is rate of erosion of the soil bed and q_s is rate of lateral sediment inflow for channels.

For upland surfaces, e is partitioned into two parts: splash erosion rate (g_s) caused by the splash of rainfall on bare soil and hydraulic erosion rate (g_h) due to the interplay between shear force of water on the loose soil bed and the tendency of soil particles to settle under the force of gravity. Splash erosion rate is approximated as a function of rainfall rate and depth of flow

$$g_s = \begin{cases} c_f k(h) r q & q > 0 \\ 0 & q < 0 \end{cases} \tag{6}$$

in which r is rainfall rate, q is rainfall excess (rainfall rate minus infiltration rate), c_f is a constant which can be estimated from the soil erodibility factor in the Universal Soil Loss Equation (USLE) (K_{usle}) as proposed by Foster et al. (1983)

$$c_f = 422 K_{usle}(\Phi_f) \tag{7}$$

with Φ_f being a reduction factor due to mulch, vegetal cover and other factors mitigating splash erosion. In Eq. (6), $k(h)$ represents the reduction in splash erosion caused by increasing depth (h) of water and is given by the empirical relation

$$k(h) = \mathrm{e}^{-c_h h} \tag{8}$$

where c_h is damping coefficient. Hydraulic erosion rate is related to the difference between equilibrium concentration and the existing sediment concentration as a kinetic transfer process

$$g_h = c_g(C_{mx} - C_s)A \tag{9}$$

Here, C_{mx} is the concentration at equilibrium transport capacity, $C_s(x,t)$ is the local sediment concentration, and c_g is a transfer rate coefficient that is estimated from USLE soil erodibility factor using the relationship proposed by Foster et al. (1983)

$$c_g = 5.6 K_{usle} \Phi_r / a_T \tag{10}$$

In Eq. (10), Φ_r is a dimensionless erosion resistance factor due to mulches or other management practices, and ranges from 0 to 1.0. In Eq. (10)

$$a_T = \begin{cases} 188 - 468 f_{cl} + 907 f_{cl}^2 & f_{cl} \le 0.22 \\ 130 & f_{cl} > 0.22 \end{cases} \tag{11}$$

where f_{cl} is a fractional clay content.

KINEROS offers several options for the sediment transport relation to estimate the transport capacity of

the flow in channels or on a plane element. The Bagnold/Kilinc sediment transport model (Kilinc and Richardson, 1973) was used in this study due to its simplicity. In this model sediment concentration is a function of local depth and hydraulic bed shear.

$$C_{mx} = \frac{C_0[u(\tau - \tau_c)]^{1.67}}{h\gamma_w u} \quad \tau > \tau_c \tag{12}$$

in which $\tau = \gamma_w hs$ with γ_w being specific weight of water, τ_c is shields critical tractive force, C_0 is a scaling parameter and u is velocity of water.

Input files required to run KINEROS were created via Arcview interface of KINEROS which has been developed by Mohammed Younus (personal communication). This interface extracts the channel network, delineates the watershed, and creates the input files necessary to run KINEROS, namely the parameter and precipitation files, using data available in GIS format. Currently, the interface can only handle runoff and consequently, estimates parameters related to runoff computation. It does not estimate any of the erosion parameters, which were entered manually. This interface is composed of 43 scripts written in Arciew Avenue language along with supplemental programs written in C language. Following steps are followed to generate input files:

1. Extracting the channel network and delineating the watershed: The only required data at this step is a DEM of the area that covers the watershed to be delineated. The TOPAZ software system (Garbrecht and Martz, 1999) was integrated with ArcView to extract topographic features from DEMs. Users need to supply CSA and minimum source channel length (MSCL). TOPAZ derives the topographic parameters of each element. For trapezoidal channel cross sections, channel bottom widths are estimated as a function of channel order based on the study of Miller et al. (1996). Subcatchment length is conceptualized as the average flow path length traveled by surface runoff from the drainage divide to the adjacent cell.
2. Overlaying the soil and land use maps over the delineated watershed: At this step KINEROS input parameters related to soil characteristics (saturated conductivity, effective net capillary drive, porosity, rock percent, etc.) and land use pattern (Manning's roughness and interception depth) are extracted. Soil data has to be in STATSGO soil format.
3. Specification of parameters that cannot be derived directly using GIS such as hydrograph duration, channel side slopes for trapezoidal channel cross sections, etc. Rainfall data has to be supplied at this step as well.
4. Preparation of parameter and precipitation files in KINEROS format.

Further details on this interface can be found in Kalin (2002).

3.1. Determination of excess rainfall

In order to minimize the number of parameters requiring calibration and to keep the analysis tractable, it was decided to first estimate excess rainfall from total rainfall. To be consistent with the KINEROS model, Smith and Parlange (1978) infiltration model was used during this study to calculate excess rainfall. They proposed the following relationship for infiltration capacity

$$f_c = K_s \frac{e^{F/B}}{e^{F/B} - 1} \tag{13}$$

where F is cumulative infiltration to time t, K_s is saturated hydraulic conductivity and

$$B = G\Phi(S_{max} - S_i) \tag{14}$$

Here Φ is the soil porosity, S_{max} and S_i are the maximum and initial values of relative saturation (= water content/porosity), respectively, and G is the effective net capillary drive given in terms of the conductivity-matric potential (Ψ) relationship

$$G = \frac{1}{K_s}\int_{-\infty}^{0} K(\Psi)\mathrm{d}\Psi \tag{15}$$

Since the infiltration rate $f = \mathrm{d}F/\mathrm{d}t$, integrating Eq. (13) with respect to time t gives

$$F = B(1 - e^{-F/B}) + K_s t \tag{16}$$

For pulsed rainfall data, cumulative infiltration and infiltration rate between times t and $t + \Delta t$ may be written as

$$F(t + \Delta t) = F(t) + B(e^{-F(t)/B} - e^{-F(t+\Delta t)/B}) + K_s t \tag{17}$$

$$f(t+\Delta t) = K_s\left(\frac{e^{F(t+\Delta t)/B}}{e^{F(t+\Delta t)/B}-1}\right) \quad (18)$$

The ponding time and cumulative infiltration at ponding are found as

$$t_p = \frac{B}{i}\ln\left(\frac{i}{i-K_s}\right) \quad i > K_s \quad (19)$$

$$F_p = it_p \quad (20)$$

where i is the rainfall intensity at a given time t.

Eqs. (17) and (18) can be solved to find infiltration and consequently excess rainfall if soil parameters B and K_s, and rainfall pattern are known. While K_s, is estimated from soil characteristics, an iterative procedure is used to calculate B by equating total direct runoff and total excess rainfall. We suspect that B is likely to be far less variable between different subwatersheds than K_s, and may be presumed as constant. This method of decoupling the infiltration process from surface flow, results in calibration of B alone, as opposed to K_{s2}, and for each element. There is some loss of physics of infiltration-flow interaction specifically during the recession phase. However, in a study on influence of geomorphologic resolution on surface runoff, Kalin and Govindaraju (2001) found that this interaction does not have a very significant effect on the results, partly because calibration accounts for some differences.

4. Model calibration

The first step was extraction of channel networks with different geomorphologic resolutions for both the study watersheds. Geomorphologic resolution is dependent on the drainage density of the channel network. This drainage density is defined as the total length of channels divided by the area of the watershed. The terms drainage density, geomorphologic resolution or just resolution are used interchangeably.

By varying the CSA (i.e. the threshold value required to initiate a channel) four different geomorphologic resolutions were obtained for each watershed. Figs. 4 and 5 depict these cases for W-2 and W-3, respectively. The number before the underscore sign (_) for each case represents the CSA

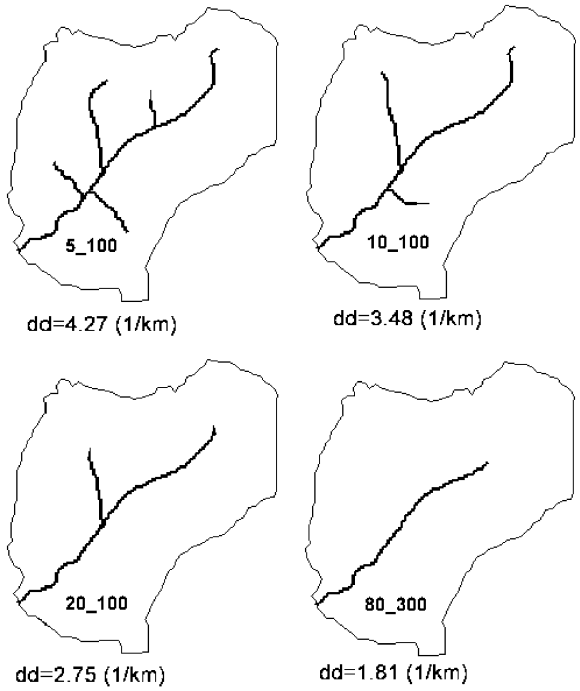

Fig. 4. Different channel network configurations for W-2.

(A_c) in hectares used during the delineation multiplied by 10. The number after the underscore sign represents the minimum length required for a first order channel in meters. For example 5_100 stands for a CSA of 0.5 hectares and a minimum channel length

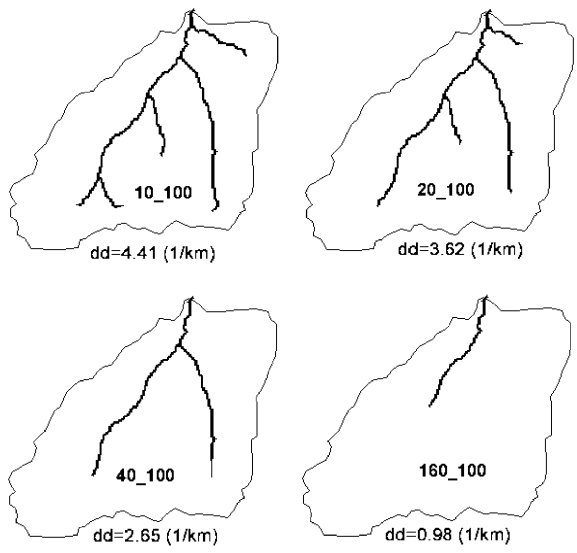

Fig. 5. Different channel network configurations for W-3.

of 100 m for first order channels. The highest and lowest resolutions are labeled as 5_100 and 80_300 for W-2. Similarly, the highest and lowest resolutions for W-3 are 10_100 and 160_100. It should be noted that these threshold values were not selected randomly. Several watershed configurations were obtained by using different threshold values. They were selected in such a way that the number of channels was different in each case and the change in drainage density was significant. The overland-flow-only case was also considered for completeness, which has zero drainage density with no channels.

Fourteen rainfall events for W-2 and 12 rainfall events for W-3 were selected for this study. The availability of appropriate runoff and sediment data that satisfied our assumption of large storm was the most important factor in selecting those events. Due to the difficulty of calculating excess rainfall with data from multiple rain gauges (although it is possible with KINEROS to use precipitation data from multiple gauges as input) each rain gauge was assigned a weight factor by forming Thiessen's polygons for each watershed to find an average rainfall pattern. The effect of rain gauge 117 is negligible with a weight factor of 0.6%. Weight factors of other gauges are very close to each other. Therefore, it was decided to use simple arithmetic averages, i.e. the rainfall data of W-2 is represented by the arithmetic average of rain gauges 115 and 116, and the rainfall data of W-3 is represented by the arithmetic average of rain gauges 112 and 113.

A total of 70 model simulations for W-2 with 5 resolutions and 14 rainfall events, and 60 simulations for W-3 with 5 resolutions and 12 rainfall events were conducted. For each geomorphologic resolution, geometric parameters of channels and overland planes were derived from the 5 m resolution DEM by ArcView-KINEROS interface. Manning's n and D_{50} were estimated from land use and soil maps, respectively, available as ArcView shape files. The erosion parameters, c_f and c_g were estimated from USLE erodibility factor, which is summarized in the Pottawattamie county, Iowa, soil survey report (Branham, 1989). Infiltration parameters were all set to zero, since excess rainfall was used as precipitation data. In fact, one of the parameters governing infiltration, B, was calibrated during computation of excess rainfall as explained in Section 3.1. The Manning's n, C_0 and D_{50} were then calibrated only for the highest resolutions in each watershed. Therefore, only events with 5_100 and 10_100 resolution were utilized during calibration for W-2 and W-3, respectively. The parameters estimated by calibration for these cases were then utilized for simulations with other resolutions. Manning's n values were calibrated first, by matching the computed peak runoffs and time to peak runoffs with observed data. Next, D_{50} values were calibrated by trying to match observed and computed time to peak sediment discharges and total sediment loads. The parameter C_0 is a scaling factor for the sedimentograph and there is no data relating it to soil information. Consequently, it is purely a calibrated parameter. It is calibrated last due to its scaling property that enables the observed and computed peak sediment discharges to be matched easily. The calibrated parameters along with the calibration targets are summarized in Table 1.

Table 1
Calibrated parameters with their targets of calibration

Calibrated parameter	Calibration target
B	Volumetric balance between excess rainfall and direct runoff
Manning's n	Peak runoff rate and time to peak
D_{50}, C_0	Time to peak sediment discharge, sediment load and peak sediment discharge

5. Results and discussion

In this paper, only a few sample results for W-2 and W-3 watersheds are shown for brevity (details available in Kalin, 2002). Some runoff hydrographs and sedimentographs are shown in Fig. 6–9 along with observed values. In each of these figures the first graph shows runoff hydrograph, and the second graph shows the sedimentograph for each resolution. Excess rainfall hyetographs computed from total rainfall, as explained in Section 3.1, are also shown in each of these figures.

In general, the KINEROS model performs fairly well although anomalies are present for some events.

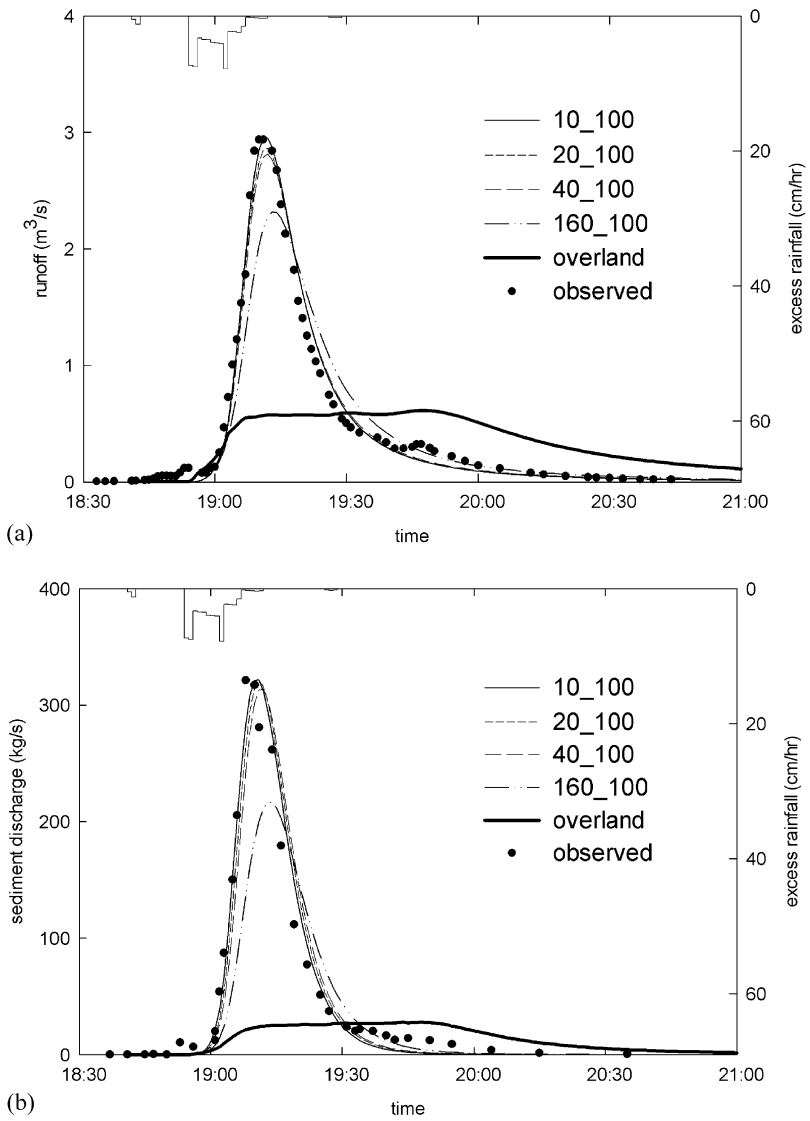

Fig. 6. Runoff hydrograph (a) and sedimentograph (b) of watershed W-2 for the rainfall event 06/13/83 with different geomorphologic resolutions.

Model performance is evaluated only for the cases with highest resolution, since calibration and parameter estimation was carried out for those cases. Computed peak runoffs and peak sediment discharges generally agree with observed values. Most discrepancies in model performance seem to occur with events having bimodal hydrographs and sedimentographs. The reason for discrepancies in some individual events might be the use of excess rainfall instead of total rainfall. It is possible to have a bimodal shape depending on the branching of the channel network and travel time distributions, but that does not appear to be the case in our study watersheds. In nature, infiltration occurs in a dynamic fashion, and continues to occur even after rainfall stops. We however assume that infiltration losses can be computed by decoupling the infiltration and surface flow processes. In some events the computed time to

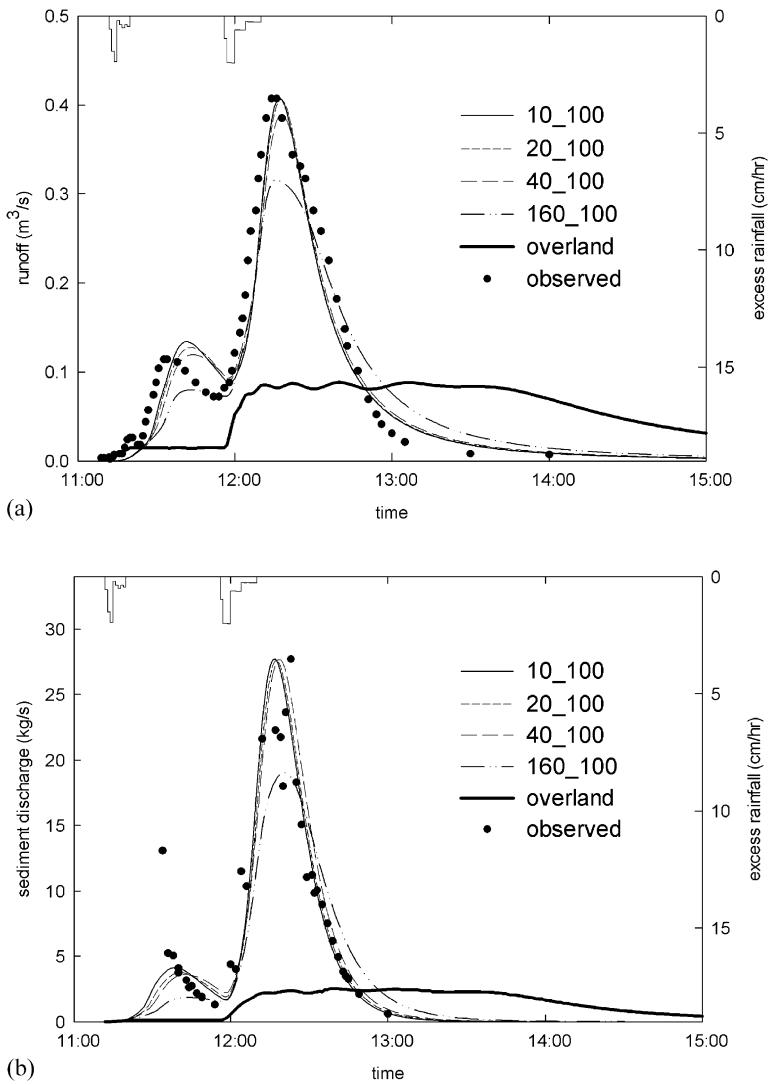

Fig. 7. Runoff hydrograph (a) and sedimentograph (b) of watershed W-2 for the rainfall event 05/30/82 with different geomorphologic resolutions.

peak runoff and time to peak sediment discharge differ significantly from the observed ones (results not shown). Based on the preceding discussion, this offset is expected in events with bimodal hydrographs.

Even for events generating unimodal hydrographs, there are discrepancies between observed and computed times to peak flow. A physical limitation of the KINEROS model is that it does not account for saturation excess overland flow. In some events, surface water movement is dictated by contributions from variable source areas close to the streams. These regions contribute to surface water before the moisture deficit over a major part of the watershed is satisfied, resulting in an earlier initiation of stream hydrograph and sedimentograph.

In general, the receding limbs of the runoff hydrographs and sedimentographs are better represented than the rising limbs. The observed

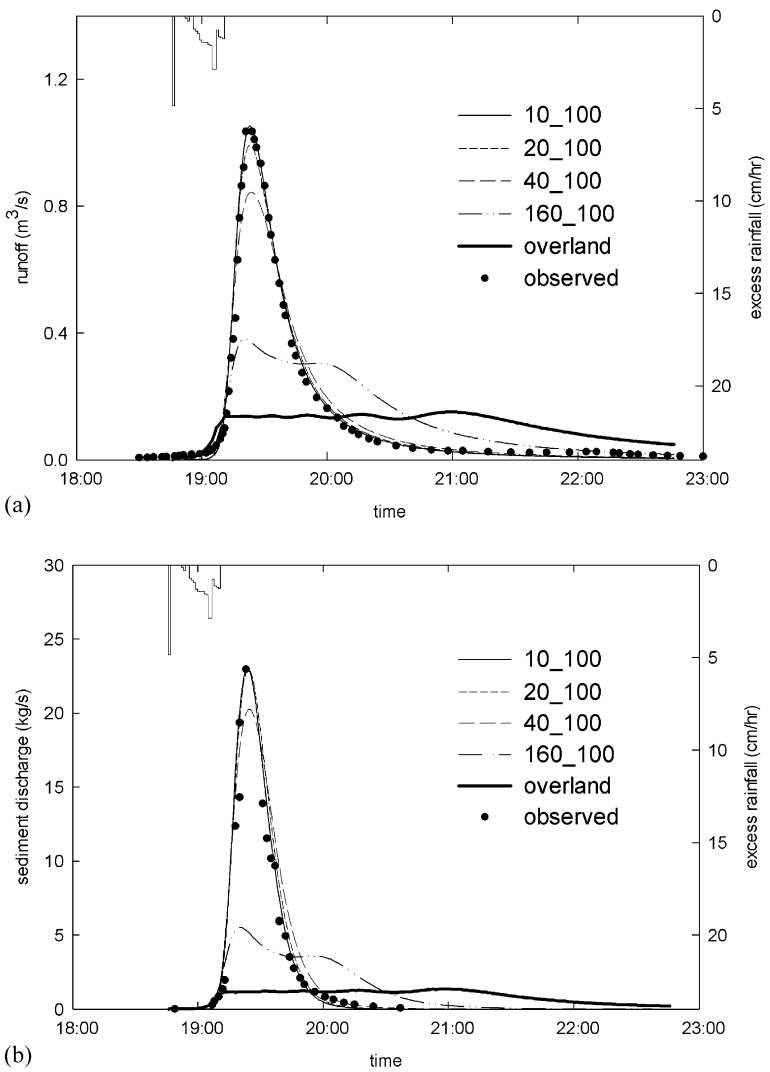

Fig. 8. Runoff hydrograph (a) and sedimentograph (b) of watershed W-3 for the rainfall event 06/13/83 with different geomorphologic resolutions.

sedimentographs are narrower than the computed ones owing to their shorter base time. As a result the total sediment load, which is the area under the sedimentograph curve, is slightly overestimated by the model.

To quantify model performance with different resolutions, an efficiency measure, R_N^2, defined by Nash and Sutcliffe (1970) was calculated as

$$R_N^2 = \frac{F_0^2 - F^2}{F_0^2} \tag{21}$$

where

$$F_0^2 = \sum (q - \bar{q})^2 \quad \text{and} \quad F^2 = \sum (q' - q)^2 \tag{22}$$

F_0^2 is the initial variance and F^2 is the index of disagreement. The quantities q and q' are the observed and computed discharges, respectively, and $\bar{q}$ is the mean of the observed discharges. The value of R_N^2 can vary from one, when there is a perfect agreement, to $-\infty$. Table 2 summarizes the R_N^2 values for several events. The Nash-Sutcliffe statistics reveal the following:

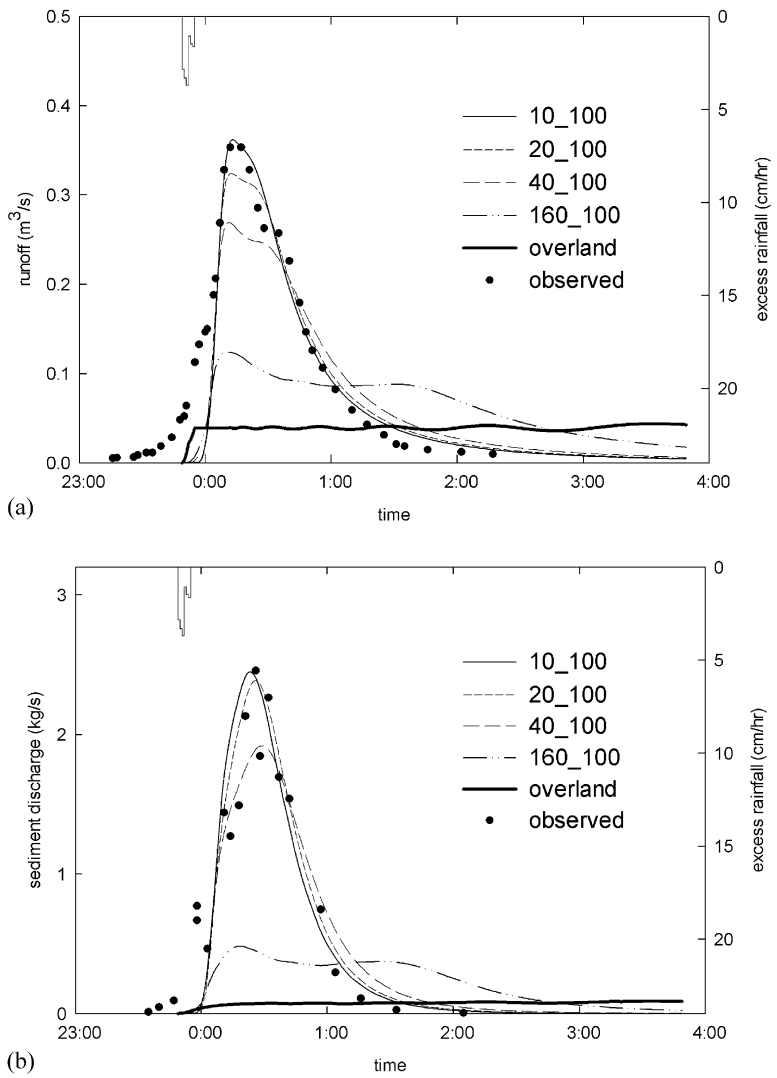

Fig. 9. Runoff hydrograph (a) and sedimentograph (b) of watershed W-3 for the rainfall event 07/03/73 with different geomorphologic resolutions.

1. The average R_N^2 for runoff values is 0.64 in W-2 and 0.48 in W-3, implying that KINEROS performs better on W-2 than it performs on W-3 in terms of simulating runoff.
2. On the other hand, the average R_N^2 for sediment discharge for W-2 is 0.38 and is 0.54 for W-3. The erosion component of KINEROS performs better on W-3 than on W-2.
3. Although a negative R_N^2 value usually means that the observed and the calculated values are likely uncorrelated, in this case negative results are often due to shifting in time between observed and calculated values. For example, if we shift the observed hydrographs and sedimentographs of the event 06/18/1980 of W-2 by 7 min to the left, we would obtain a very good match. However, the R_N^2 values obtained for runoff and sediment discharge are -0.464 and -1.508, respectively. The possible reasons that might cause these anomalies were discussed previously.

Table 2
Summary of Nash–Sutcliffe R_N^2 values for W-2 and W-3

W-2			W-3		
Event	R_N^2		Event	R_N^2	
	Runoff	Sediment		Runoff	Sediment
6/13/1983	0.984	0.973	8/12/1986	0.533	0.189
9/17/1982	0.614	−0.051	6/12/1984	0.131	0.418
6/30/1982	0.859	0.779	5/25/1984	0.829	0.631
6/15/1982	0.893	0.796	6/13/1983	0.982	0.962
6/14/1982	0.821	0.744	8/1/1981	0.893	0.863
5/30/1982	0.913	0.837	7/18/1981	0.330	0.167
8/26/1981	−0.587	−1.208	6/7/1980	−0.473	0.257
8/1/1981	0.969	0.764	6/4/1980	0.782	0.893
7/8/1981	0.948	0.891	5/28/1978	0.224	0.676
9/5/1980	0.264	−0.287	5/19/1978	0.574	0.512
6/18/1980	−0.464	−1.508	6/27/1976	0.262	0.155
6/12/1980	0.944	0.904	7/3/1973	0.719	0.746
8/15/1977	0.834	0.725			
8/29/1975	0.943	0.976			

5.1. Effect of resolution on runoff hydrograph

The runoff hydrographs in Figs. 6–9 show that as the geomorphologic resolution decreases the peak runoff decreases too. In other words, the highest resolution generates the highest peak runoff. In contrast, time to peak does not change appreciably with increasing resolution, except for the pure overland flow case where time to peak is very large as expected. According to Munoz-Carpena et al. (1993) time to peak primarily depends on the ponding time, which is affected by soil properties. Since we eliminated infiltration effects by using excess rainfall, time to peak remains almost constant with changing resolution. Increasing geomorphologic resolution results in an increase in the total length of channels and a corresponding decrease in characteristic length of overland flow planes, resulting in higher peaks. Another observation is the strong tails in the receding limbs of the hydrographs with decreasing resolution. This is a result of decreasing peak runoff with decreasing resolution combined with the fact that the total volume of runoff is the same for each resolution due to no infiltration.

It is clear from Figs. 6–9 that as the drainage density increases the differences between peak runoffs and the entire hydrograph become smaller suggesting a limiting value for the peak runoff. In other words, further increase in drainage density does not cause a significant change in peak runoff on the hydrograph at the basin outlet. This effect can be better observed in Fig. 10, where the peak runoffs are plotted against the drainage densities. In the figure, hollow circles represent the average peak runoffs for each drainage density.

Based on these observations, a relation between drainage density, watershed area and peak runoff was sought. We fit a mathematical function to estimate the runoff rates if simulations with higher drainage densities had been performed. According to this model, the peak runoff at a certain resolution (indicated by the drainage density) is given by

$$q = q_0 + (q_{peak} - q_0)(1 - e^{-k^* dd}) \quad (23)$$

where q is peak runoff corresponding to certain level of geomorphologic resolution, dd is drainage density, k is a fitting parameter, q_0 is peak runoff when dd = 0 (pure overland flow case) and q_{peak} is asymptotic peak discharge.

Using the computed peak runoffs for each rainfall event with different resolutions, q_{peak} and k values were found by fitting Eq. (23). Tables 3 and 4 summarize the parameters q_{peak} and k estimated for W-2 and W-3, respectively. The R^2 values are also given to evaluate model performance. The parameter k in Eq. (23) can be thought as one-third of the drainage density that is required to produce a hydrograph that can be improved by only 5% or less with further increase in geomorphologic resolution.

It is desirable to develop a general expression relating resolution of the channel network to the basin characteristics and climatic properties so that it will be applicable to similar watersheds subjected to different rainfall conditions. In order to find such a relationship, peak discharges, calculated for each resolution and rainfall event were non-dimensionalized by dividing with the corresponding asymptotic q_{peak} values what would likely be obtained for infinitely high resolution and were estimated by Eq. (23) and tabulated in Tables 3 and 4. This new non-dimensional runoff is denoted by q^*. The q^* values corresponding to same rainfall pattern and same geomorphologic resolution were plotted against a new dimensionless number r,

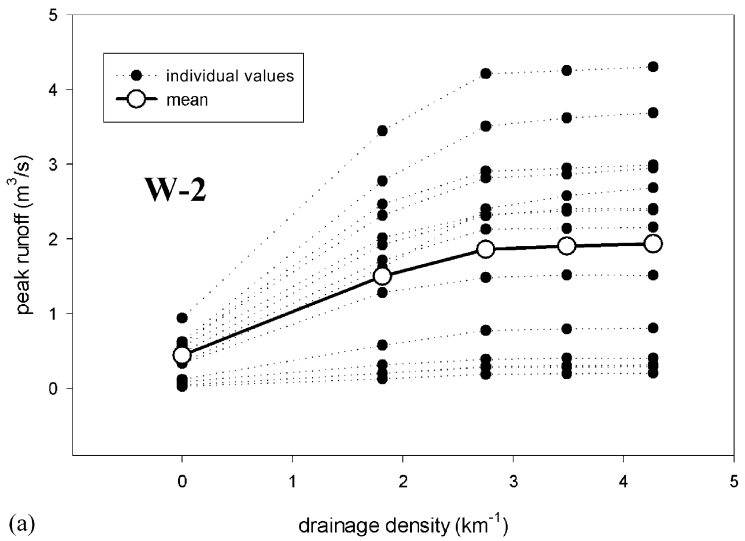

Fig. 10. Peak runoffs plotted against drainage density.

defined as D^*dd, where D is the total excess rainfall depth, to see if a relation could be deduced between these two dimensionless quantities. The variable r may also be expressed as $r = i_{max}\Delta t(\text{dd})$, where i_{max} is the maximum excess rainfall intensity and Δt is a time interval chosen such that the product $i_{max}\Delta t$ is equal to D, the total rainfall depth. A curve was fitted to the plotted data (Fig. 11) under the constraints that $q^*(0) = 0$, and $q^*(\infty) = 1$. When there is no rain $D = 0$ and consequently $r = 0$, implying that q^* has to be zero. Similarly when r is asymptotically infinite, q^* is one. The fitted equation is

$$q^* = 1 - e^{-164830r} \tag{24}$$

with an R^2 value of 0.61.

Eq. (24) can be utilized for determining the appropriate geomorphologic resolution that would lead to acceptable results. Upon deciding on an acceptable level for q^* (say 0.95 for instance) we could solve for r and consequently determine

Table 3
Fitted parameters for W-2 defined in Eq. (23)

Event	Observed runoff (m^3/s)	Peak runoffs for given resolutions (m^3/s)					q_{peak} (m^3/s)	k	R^2
		5_100 (dd = 4.27 km^{-1})	10_100 (dd = 3.48 km^{-1})	20_100 (dd = 2.75 km^{-1})	80_300 (dd = 1.81 km^{-1})	Overland (dd = 0.00 km^{-1})			
06/13/1983	2.938	2.950	2.865	2.817	2.316	0.612	3.130	0.663	0.997
09/17/1982	0.305	0.313	0.303	0.293	0.202	0.043	0.383	0.405	0.983
06/30/1982	2.150	2.157	2.142	2.130	1.716	0.425	2.296	0.710	0.999
06/15/1982	0.802	0.805	0.795	0.775	0.578	0.121	0.907	0.543	0.989
06/14/1982	4.274	4.303	4.254	4.211	3.446	0.941	4.561	0.705	0.994
05/30/1982	0.407	0.408	0.406	0.389	0.315	0.088	0.444	0.605	0.995
08/26/1981	0.203	0.205	0.197	0.188	0.129	0.027	0.259	0.372	0.985
08/01/1981	2.938	2.990	2.947	2.906	2.466	0.602	3.111	0.790	0.998
07/08/1981	2.382	2.384	2.370	2.331	2.015	0.558	2.470	0.833	0.998
09/05/1980	0.293	0.294	0.283	0.283	0.203	0.044	0.336	0.499	0.984
06/18/1980	2.404	2.407	2.405	2.311	1.922	0.473	2.564	0.692	0.997
06/12/1980	3.707	3.688	3.620	3.509	2.777	0.627	4.024	0.599	0.995
08/15/1977	2.666	2.684	2.579	2.401	1.617	0.340	3.633	0.315	0.993
08/29/1975	1.503	1.513	1.519	1.482	1.283	0.334	1.572	0.844	0.998

the drainage density that is required to achieve this level of accuracy in estimating the peak discharge. In fact, minimum required drainage density (dd) may be expressed in turns of q^* directly as

$$\mathrm{dd} = \frac{1}{164830D}\ln\left(\frac{1}{1-q^*}\right) \quad (25)$$

By knowing the total excess precipitation (D), say for a design storm, and q^* in advance, the required drainage density could be determined using Eq. (25). Table 5 shows minimum required drainage densities calculated using Eq. (25) for some selected D and q^* values. For example, with $D = 10$ mm, the resolution represented by only one channel segment (a drainage

Table 4
Fitted parameters for W-3 defined in Eq. (23)

Event	Observed runoff (m^3/s)	Peak runoffs for given resolutions (m^3/s)					q_{peak} (m^3/s)	k	R^2
		10_100 (dd = 4.41 km^{-1})	20_100 (dd = 3.62 km^{-1})	40_100 (dd = 2.65 km^{-1})	160_300 (dd = 0.98 km^{-1})	overland (dd = 0.00 km^{-1})			
08/12/1986	1.403	1.403	1.374	1.231	0.574	0.235	1.825	0.336	0.992
06/12/1984	0.211	0.195	0.187	0.162	0.075	0.030	0.276	0.273	0.995
05/25/1984	0.193	0.205	0.189	0.157	0.074	0.042	0.464	0.117	0.996
06/13/1983	1.035	1.054	0.993	0.843	0.382	0.151	1.636	0.226	0.996
08/01/1981	1.971	1.949	1.953	1.847	0.990	0.480	2.275	0.455	0.990
07/18/1981	0.745	0.745	0.730	0.656	0.309	0.133	0.968	0.335	0.992
06/07/1980	0.679	0.683	0.671	0.580	0.269	0.107	0.934	0.300	0.994
06/04/1980	1.532	1.709	1.697	1.552	0.784	0.337	2.083	0.398	0.992
05/28/1978	0.882	0.889	0.854	0.738	0.340	0.132	1.254	0.276	0.995
05/19/1978	0.816	0.819	0.817	0.740	0.353	0.150	1.030	0.371	0.991
06/27/1976	2.795	2.810	2.765	2.549	1.242	0.574	3.505	0.370	0.991
07/03/1973	0.353	0.362	0.324	0.269	0.124	0.044	0.686	0.159	0.999

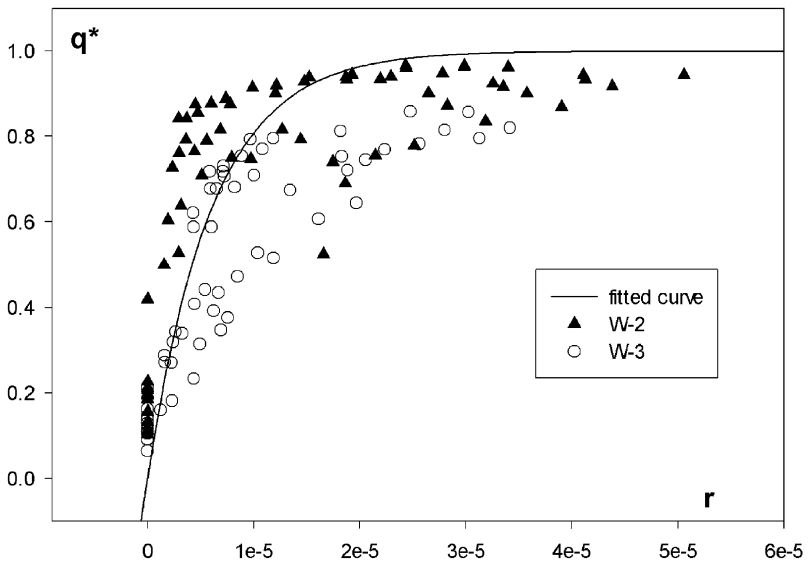

Fig. 11. Plot of dimensionless discharge (q^*) versus r.

density of 1.81 km^{-1}) is sufficient to achieve a q^* of 0.95 for the W-2 watershed. With the same D value, the required drainage density for W-3 is 2.794 km^{-1} if a q^* value of 0.99 is desired. This resolution corresponds to the case represented by 40_100 that has a drainage density of 2.65 km^{-1}.

5.2. Effect of resolution on sedimentograph

The trend in variation of peak sediment discharges with increasing geomorphologic resolution is different from the trend observed in peak runoff rates. Our results suggest anomalous behavior in that the highest resolution does not necessarily generate the highest sediment discharge. This can be seen in plots of sediment discharge versus time for different resolutions (Figs. 6–9). The general trend in both watersheds is that peak sediment discharge initially increases with increasing resolution. However, after a threshold resolution has been reached it starts decreasing with increasing resolution. In W-2, a resolution of 5_100 generates the highest peak sediment discharge in 7 of the 14 events and 10_100 generates the highest peak in the remaining seven events. It appears that the threshold resolution for W-2 is in between 5_100 and 10_100, which corresponds to an average drainage density of 3.90 km^{-1}. For W-3, 20_100 results in the highest peak in 7 of the 12 events, 10_100 in 2 of them, and 40_100 has the highest peak in only one event. In two events 10_100

Table 5
Minimum drainage densities required for the given q^* and total precipitations

Total excess precipitation, D, (mm)	q^*				
	0.999	0.99	0.98	0.95	0.90
1	41.908	27.939	23.734	18.175	13.969
5	8.382	5.588	4.747	3.635	2.794
10	4.191	2.794	2.373	1.817	1.397
20	2.095	1.397	1.187	0.909	0.698
30	1.397	0.931	0.791	0.606	0.466
40	1.048	0.698	0.593	0.454	0.349
50	0.838	0.559	0.475	0.363	0.279

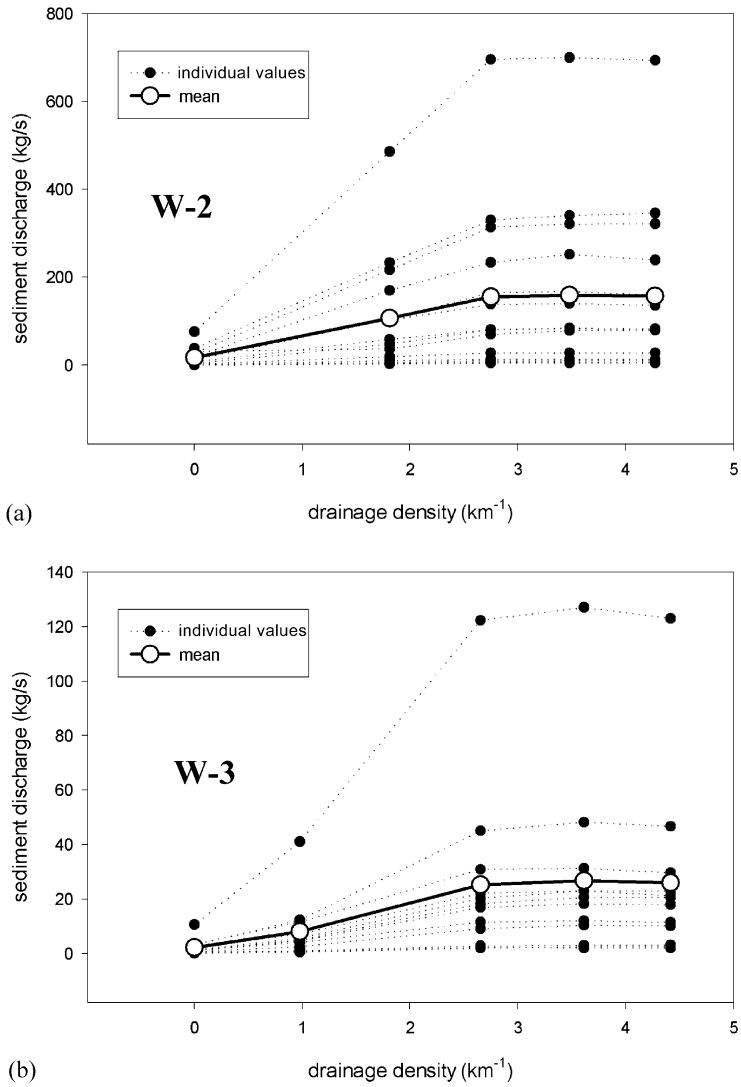

Fig. 12. Peak sediment discharges plotted against drainage density.

and 20_100 share the highest peaks. The threshold for W-3 lies in between 10_100 and 20_100 and is closer to 20_100. Using the number of events generating the highest peak for each resolution as the weight factor results in an average drainage density of 3.74 m^{-1}, close to the value obtained for W-2. The effect of resolution on peak sediment discharge can also be seen in Fig. 12, where drainage densities are plotted against peak discharges for the two watersheds. Again, the open circles denote the average values for a given drainage density.

Effect of geomorphologic resolution on total sediment load, which is the total amount of sediment accumulated at the watershed outlet, was also examined. Total sediment loads at the watershed outlet for each event and resolution were computed and plotted against drainage density (Fig. 13). The trend was similar to the one observed when studying peak discharge values. In this case, the required resolution for W-2 falls in between 10_100 and 20_100 with a drainage density of 3.26 km^{-1}, as compared to 3.90 km^{-1} when peak sediment

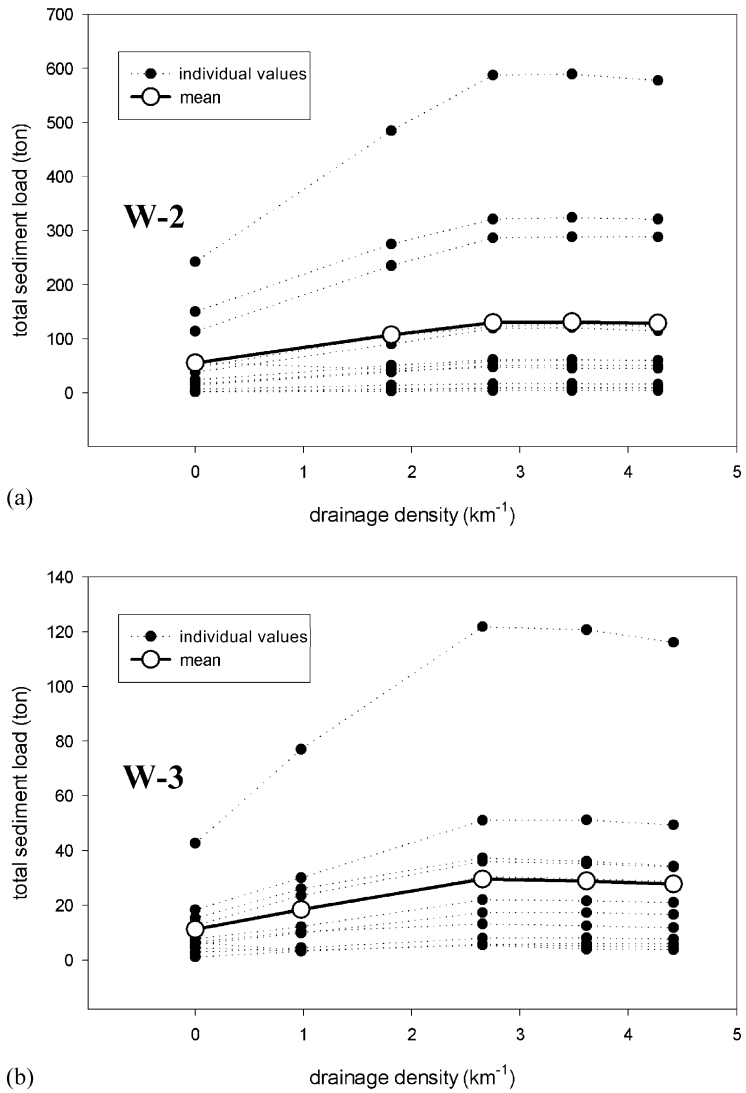

Fig. 13. Total sediment loads at the watershed outlet plotted against drainage density.

discharges were considered. For W-3 the corresponding threshold values of drainage density are 2.97 km^{-1} for sediment volume as compared to 3.74 km^{-1} for peak discharge. This resolution falls in between 20_100 and 40_100.

The reason for this anomalous behavior for sediment discharge hydrographs is explained as follows. Increasing the drainage density increases the number of channels and more importantly causes the channel heads to move upward resulting in an increase in total length of channels. At the same time the characteristic lengths of overland flow planes gets smaller. If the length of the overland plane is not long enough, sediment concentration may not attain its equilibrium value. In that case, no deposition can be expected. On the contrary, in channel segments the sediment coefficients c_f, c_h and C_0 are all set to zero. This means splash erosion is ignored in channels. In our simulations, the dominant process in the channels is not erosion but deposition. Therefore, starting from pure overland flow, increasing resolution first increases sediment discharge and total sediment load

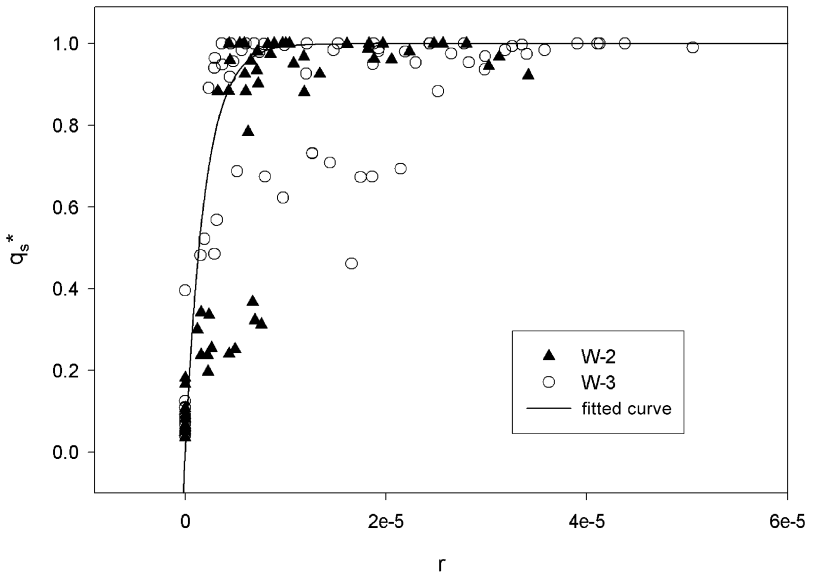

Fig. 14. Plot of dimensionless sediment discharge (q_S^*) versus r.

since we expect less deposition on the overland planes. This continues until some threshold resolution is reached. After that point, in most overland flow planes, the effect of deposition vanishes and we might expect almost a constant amount of sediment to be delivered to the channels. However, deposition increases in the channel segments due to the increase in the total length of channels and this causes a decrease in sediment discharge and total sediment load.

For each rainfall event, peak sediment discharges obtained for different resolutions were divided with the highest sediment discharge value of that particular event. We call these dimensionless sediment

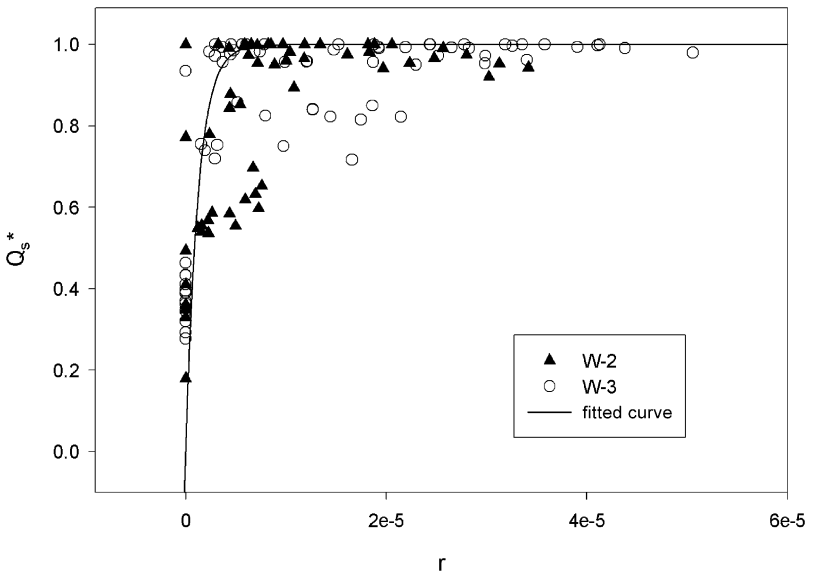

Fig. 15. Plot of dimensionless total sediment loads (Q_S^*) versus r.

discharges as q_s*. Total sediment loads observed at the watershed outlet were also non-dimensionalized in a similar manner and named Q_s*. We plotted these dimensionless sediment discharges and sediment loads against r which was defined as the product of excess rainfall depth and drainage density (Figs. 14 and 15). A curve in the form of Eq. (24) was fitted to the data with R^2 values of 0.76 for dimensionless sediment discharges and 0.21 for dimensionless total sediment loads. The reason for having the very low R^2 value in Fig. 15 for total sediment load is the unusual response observed for the event 06/12/1984 over W-3. Unlike the general trend, the maximum total load corresponds to the lowest resolution, i.e. pure overland flow for this event. The triangle on the upper left corner of Fig. 15 that corresponds to $r = 0$ and $Q_s* = 1$, represents this data point. Removing some of these outliers would cause a dramatic improvement in the R^2 statistics. The fitted equations for dimensionless peak sediment discharges and total sediment loads, respectively, are

$$q_s* = 1 - e^{-316680r} \tag{26}$$

$$Q_s* = 1 - e^{-532340r} \tag{27}$$

Eqs. (26) and (27) can be used to determine minimum drainage density required to achieve a desired accuracy. We need to know in advance D and decide on q_s* or Q_s*, depending on the quantity of interest, to estimate the minimum required drainage density.

6. Summary and conclusions

Physically based models of surface hydrology often prove to be ineffective because huge amounts of data are required to use such models at their full potential. Even if such data were available or could be generated, prohibitive computational effort would be required in simulation of different scenarios that would lead to a good understanding of the surface hydrology. Computational costs are directly dependent on the level of spatial resolution (detail) incorporated into the model. The question of finding the right degree of discretization—one that sufficiently captures the important features of the solution while entailing minimal computational effort—has still not been addressed satisfactorily and is the focus of this paper.

We find that the optimal geomorphologic resolution depends on the quantity of interest. Among the quantities considered here, the required geomorphologic resolution is highest when the peak runoff is of main concern and is lowest when the total sediment load at the watershed outlet is the quantity of interest. The required resolution is in between these two cases when the focus is on peak sediment discharge.

Peak runoff has a different trend with varying resolution compared to peak sediment discharge and total sediment volume. As the drainage density increases peak runoff increases too. However, after some optimal resolution the differences between peak runoff rates become insignificant. This motivated us to develop an empirical relationship between drainage density, total excess precipitation and maximum peak discharge which could be used to estimate the minimum required drainage density given the total excess rainfall. Goodrich et al. (1988) claimed that such simplifications are only possible for big rainfall events ($T_r > 2.8$ years) when peak runoff is concerned. Our results support this argument as they indicate that a lower geomorphologic resolution is adequate to achieve desired accuracy in peak discharge for larger rainfall events.

In this study, two watersheds with similar topographic and climatic characteristics were used. It would appear that the observed trends will hold true for other small watersheds with different topographic characteristics under different climatic conditions. The quantitative results of this study are perhaps specific to these watersheds and to the KINEROS model. As there is no accepted or 'universal' model for erosion at the watershed scale, no conclusive statement can be made in this regard.

This study was geared towards large storms. Small storms result in different effects, such as eroded sediment not reaching the watershed outlet, and deposition in swale bottoms. We assumed that these would have negligible influence on our results.

The quality of data is always of concern, especially for model calibration. The sediment data is more suspect in this regard. The available form of data for sediment in this study was sediment concentrations given in parts per million (ppm). To calculate sediment discharges sediment concentrations were multiplied with measured flow discharges. This involved some interpolation, since the time of measurements for

sediment concentrations and flow discharges did not always match. While this would influence estimates of calibration parameters, the trends indicated by model and observed results are quite realistic. The findings of this study might be further verified through various other models, though we believe that the general trends revealed from the analysis would hold more universally for other models.

Acknowledgements

This research was funded by EPA, Award No. R-82833901-0. The authors acknowledge this support. Special thanks to Larry Kramer, USDA-ARS-NSTL-DLRS, Council Bluffs, IA, for supplying all the data sets. The paper benefited from the constructive review comments of M.J. Kirkby and R.E. Smith.

References

Amorocho, J., 1961. Discussion on 'Predicting storm runoff on small experimental watershed' by N.E. Minshall'. Journal of Hydraulics Division, ASCE 87 (HY2), 185–191.

Beven, K., Kirkby, M.J., 1979. A physically based, variable contributing area model of basin hydrology. Hydrological Sciences Bulletin 24, 43–69.

Bingner, R.L., Garbrecht, J., Arnold, J.G., Srinivasan, R., 1997. Effect of watershed subdivision on simulation runoff and fine sediment yield. Transactions of ASAE 40 (5), 1329–1335.

Bloschl, G., Sivapalan, M., 1995. Scale issues in hydrological modeling: a review. Hydrological Processes 9, 251–290.

Branham, C.E., 1989. Soil Survey of Pottawattamie County, Iowa, US Department of Agriculture, Washington, DC.

Bruneau, P., Gascuel-Odoux, C., Robin, P., Merot, P., Beven, K., 1995. Sensitivity to space and time resolution of a hydrological model using digital elevation data. Hydrological Processes 9, 69–81.

Chung, S.W., Gassman, P.W., Kramer, L.A., Williams, J.R., Gu, R., 1999. Validation of EPIC for two watersheds in southwest Iowa. Journal of Environmental Quality 28 (3), 971–979.

Corradini, C., Melone, F., Ubertini, L., Singh, V.P., 1986. Geomorphologic approach to synthesis of direct runoff hydrograph from the Upper Tiber basin, Italy'. In: Gupta, V.K., Rodriguez-Iturbe, Wood, E.F. (Eds.), Scale Problems in Hydrology,.

Da Ros, D., Borga, M., 1997. Use of digital elevation model data for the derivation of the geomorphological instantaneous unit hydrograph. Hydrological Processes 11, 13–33.

Foster, G.R., Smith, R.E., Knisel, W.G., Hakonson, T.E., 1983. Modeling the effectiveness of on-site sediment controls', paper 83-2092, presented at the summer 1983 meeting, ASAE, Bozeman, MT, p. 15.

Gandolphi, C., Bischetti, G.B., 1997. Influence of the drainage network identification method on geomorphological properties and hydrological response. Hydrological Processes 11, 353–375.

Garbrecht, J., Martz, L.W., 1996. Comment on: digital elevation model grid size, landscape representation, and hydrologic simulations by Weihua Zhang and David R. Montgomery. Water Resources Research 32, 1461–1462.

Garbrecht, J., Martz, L.W., 1999. An automated digital landscape analysis tool for topographic evaluation, drainage identification, watershed segmentation, and subcatchment parameterization, Rep.# GRL 99-1, Grazinglands Research Laboratory, USDA, Agricultural Research Service, El Reno, OK.

Goodrich, D.C., 1992. An overview of the USDA-ARS climate change and hydrology program and analysis of model complexity as a function of basin scale, Proceedings of the Workshop on the Effects of Global Climate Change on Hydrology and Water Resources at a Catchment Scale, 233–242, Tsukuba, Japan, 3–6 Feb,.

Goodrcih, D.C., Woolhiser, D.A., Sorooshian, S., 1988. Model complexity required to maintain hydrologic response, Proceedings of ASCE National Conference on Hydraulic Engineering, Colorado Springs, Colo., 6–12 Aug, pp. 431–436.

Helmlinger, K.R., Kumar, P., Foufoula-Georgiou, E., 1993. On the use of digital elevation model data for Hortonian and fractal analyses of channel networks. Water Resources Research 29, 2599–2613.

Kalin, L., 2002. Sediment source area identification over watersheds: influence of spatial scale and sediment travel times, PhD Dissertation, Purdue University, W. Lafayette, IN.

Kalin, L., Govindaraju, R.S., 2001. Influence of GIS resolution on response in the stream, Proceedings of World Water and Environmental Congress, 20–24 May, Orlando, FL.

Karlen, D.L., Kramer, L.A., 1991. Balancing corn yield goals and N fertilization rates. Proceedings of New Technology in Agriculture, 1991 Crop Production and Protection Conference, Iowa State University: Ames, IA, 227–235.

Karlen, D.L., Kramer, L.A., Logsdon, S.D., 1998. Field-scale nitrogen balances associated with long-term continuous corn production. Agronomy Journal 90, 644–650.

Kilinc, M., Richardson, E.V., 1973. Mechanics of soil erosion from overland flow generated by simulated rainfall, Hydrology Paper 63, p. 54, Colorado State University, Fort Collins.

Kirkby, M.J., 1988. Hillslope runoff process and models. Journal of Hydrology 100, 315–339.

Kramer, L.A., Alberts, E.E., Hjelmfelt, A.T., Gebhardt, M.R., 1990. Effect of soil conservation systems on groundwater nitrate levels from three corn-cropped watersheds in southwest Iowa. In: Lehr, J., (Ed.), Proceedings of the 1990 Cluster of Conferences, Kansas City, MO, 20–21 Feb. 1990, National Ground Water Association, Westerville, OH, 1990., pp. 175–189.

Miller, S.N., Guertin, D.P., Goodrich, D.C., 1996. Investigating stream channel morphology using a geographic information system, ESRI User Conference, 1996, San Diego, CA,.

Miller, S.N., Guertin, D.P., Kamran, H.S., Goodrich, D.C., 1999. Using high resolution synthetic aperture radar for terrain mapping: Influences on hydrologic and geomorphic investigation, Proceedings of Wildland Hydrology, AWRA Summer Specialty Conference, Bozeman, Montana,.

Minshall, N.E., 1960. Predicting storm runoff on small experimental watersheds. Journal of Hydraulics Division, ASCE 86 (HY8), 17–38.

Montgomery, D.R., Dietrich, W.E., 1988. Where do channels begin? Nature 336, 232–234.

Montgomery, D.R., Foufoula-Georgiou, E., 1993. Channel network source representaion using digital elevation models. Water Resources Research 25, 1907–1918.

Moore, I.D., O'Louglin, E.M., Burch, G.J., 1988. A contour-based topographic model for hydrological and ecological applications. Earth Surface Process Landforms 13, 305–320.

Morris, G.D., Heerdegen, R.G., 1988. Automatically derived catchment boundaries and channel networks and their hydrological applications. Geomorphology 1, 131–141.

Munoz-Carpena, R., Parsons, J.E., William, J.W., 1993. Numerical approach to the overland flow process in vegetative filter strips. Transactions of ASAE 36, 761–770.

Nash, J.E., Sutcliffe, J.V., 1970. River flow forecasting through conceptual models, I-A discussion of principles. Journal of Hydrology 10, 282–290.

Norris, G.R., 1992. A process for interfacing a hydrologic model to a geographic information system, MS Thesis, Department of Agricultural Engineering, Oklahoma State University, Stillwater.

Norris, G.R., Haan, C.T., 1993. Impact of subdividing watersheds on estimated hydrographs. Applied Engineering in Agriculture 9 (5), 443–445.

Rigon, R., Rinaldo, A., Rodriguez-Iturbe, I., Bras, R.L., Ijjasz-Vasquez, E., 1993. Optimal channel networks: a frame-work for the study of river basin morphology. Water Resources Research 29 (6), 1635–1646.

Rinaldo, A., Rodriguez-Iturbe, I., Rigon, R., Bras, R.L., Ijjasz-Vasquez, E., Marani, A., 1992. Minimum energy and fractal structures of drainage networks. Water Resources Research 28 (9), 2183–2195.

Rinaldo, A., Vogel, G.K., Rigon, R., Rodriguez-Iturbe, I., 1995. Can one gauge the shape of a basin? Water Resources Research 31, 1119–1127.

Rodriguez-Iturbe, I., Ijjasz-Vasquez, E., Bras, R.L., Tarboton, D.G., 1992. Power law distribution of mass and energy in river basins. Water Resources Research 28 (4), 1089–1093.

Smith, R.E., Parlange, J.Y., 1978. A parameter-efficient hydrologic infiltration model. Water Resources Research 14 (3), 538–553.

Snell, J.D., Sivapalan, M., 1994. On the geomorphologic dispersion in natural catchments and geomorphological unit hydrograph. Water Resources Research 30, 2311–2323.

Steinheimer, T.R., Scoggin, K.D., Kramer, L.A., 1998a. Agricultural chemical movement through a field-size watershed in Iowa: subsurface hydrology and distribution of nitrate in groundwater. Environmental Science and Technology 32, 1039–1047.

Steinheimer, T.R., Scoggin, K.D., Kramer, L.A., 1998b. Agricultural chemical movement through a field-size watershed in Iowa: surface hydrology and nitrate losses in discharge. Environmental Science and Technology 32, 1048–1052.

Tarboton, D.G., Ames, D.P., 2001. Advances in the mapping of flow networks from digital elevation data, Proceedings of the World Water and Environmental Resources Congress, ASCE, Orlando, FL, May,.

Tarboton, D.G., Bras, R.L., Rodriguez-Iturbe, I., 1988. The fractal nature of river networks. Water Resources Research 24 (8), 1317–1322.

Tarboton, D.G., Bras, R.L., Rodriguez-Iturbe, I., 1991. On the extraction of channel networks from digital elevation data. Hydrological Processes 5, 81–100.

Thieken, A.H., Lucke, A., Diekkruger, B., Richter, O., 1999. Scaling input data by GIS for hydrological modelling. Hydrological Processes 13, 611–630.

Vieux, B., Needham, S., 1993. Nonpoint-pollution model sensitivity to grid cell size. Journal of Water Resources Planning and Management 119, 141–157.

Woolhiser, D.A., Smith, R.E., Goodrich, D.C., 1990. KINEROS–a kinematic runoff and erosion model: documentation and user manual. US Department of Agriculture, Agricultural Research Service, ARS-77, 130.

Zhang, W., Montgomery, D.R., 1994. Digital elevation model grid size, landscape representation, and hydrologic simulations. Water Resources Research 30, 1019–1028.